PCCP

RSC Publishing

PAPER

View Article Online
View Journal | View Issue

Cite this: *Phys. Chem. Chem. Phys.*, 2013, **15**, 13108

Design and biophysical characterization of atrazine-sensing peptides mimicking the *Chlamydomonas reinhardtii* plastoquinone binding niche

Viviana Scognamiglio,[a] Pasquale Stano,[b] Fabio Polticelli,[bc] Amina Antonacci,[a] Maya Dimova Lambreva,[a] Giorgio Pochetti,[a] Maria Teresa Giardi[a] and Giuseppina Rea*[a]

Received 8th May 2013,
Accepted 2nd June 2013

DOI: 10.1039/c3cp51955d

www.rsc.org/pccp

The plastoquinone (Q_B) binding niche of the Photosystem II (PSII) D1 protein is the subject of intense research due to its capability to bind also anthropogenic pollutants. In this work, the *Chlamydomonas reinhardtii* D1 primary structure was used as a template to computationally design novel peptides enabling the binding of the herbicide atrazine. Three biomimetic molecules, containing the Q_B-binding site in a loop shaped by two α-helices, were reconstituted by automated protein synthesis, and their structural and functional features deeply analysed by biophysical techniques. Standing out among the others, the biomimetic mutant peptide, D1pepMut, showed high ability to mimic the D1 protein in binding both Q_B and atrazine. Circular dichroism spectra suggested a typical properly-folded α-helical structure, while isothermal titration calorimetry (ITC) provided a complete thermodynamic characterization of the molecular interaction. Atrazine binds to the D1pepMut with a high affinity (K_d = 2.84 μM), and a favourable enthalpic contribution ($\Delta H = -11.9$ kcal mol^{-1}) driving the interaction. Fluorescence spectroscopy assays, in parallel to ITC data, provided hyperbolic titration curves indicating the occurrence of a single atrazine binding site. The binding resulted in structural stabilisation of the D1pepMut molecule, as suggested by atrazine-induced cooperative profiles for the fold–unfold transition. The interaction dynamics and the structural stability of the peptides in response to the ligand were particularly considered as mandatory parameters for biosensor/biochip development. These studies paved the way to the set-up of an array of synthetic mutant peptides with a wide range of affinity towards different classes of target analytes, for the development of optical nanosensing platforms for herbicide detection.

Highlights

• Novel biomimetic peptides of the photosynthetic plastoquinone binding niche were designed by exploring the D1 primary structure of *Chlamydomonas reinhardtii*.

• Circular dichroism, fluorescence spectroscopy and microcalorimetry experiments addressed the biophysical and structural properties of the novel produced bio-inspired molecules.

• The redefined more hydrophilic peptide sequence of D1pepMut adopted a properly-folded α-helical structure.

• D1pepMut had the ability to bind either plastoquinone or atrazine.

• Atrazine binding to D1pepMut enhances the peptide structural stability.

Introduction

The photosynthetic membranes host macromolecular assemblies of enzymes and pigments enabling plants, cyanobacteria and algae to sustain life on Earth.[1] Acting as a light-driven water:plastoquinone oxidoreductase, the Photosystem II (PSII) entraps light energy by the chlorophyll–protein harvesting complexes and transfers it to the active reaction center dominated by the D1–D2 heterodimer and oxygen evolving complex. The absorbed excitons induce a charge separation in a special dimer of Chl *a* molecules generating a single electron transfer towards a pheophytin molecule, then to a plastoquinone molecule in D2, Q_A, and finally, to a second plastoquinone in D1, Q_B. The electron transfer chain rounds out beyond the PSII, leading

[a] *Institute of Crystallography, CNR, Via Salaria km 29.3, Monterotondo, 00015 Rome, Italy. E-mail: giuseppina.rea@mlib.ic.cnr.it*
[b] *Department of Sciences, University Roma Tre, 00146 Rome, Italy*
[c] *National Institute of Nuclear Physics, Roma Tre Section, 00146 Rome, Italy*

to the final production of reducing equivalents and molecular oxygen.[2,3]

The highly homologous D1 and D2 proteins stand out at the heart of the PSII core complex interacting with all the redox cofactors involved in the charge separation and electron transport across the membrane. Since its discovery, the chloroplastic *psb*A gene-encoded D1 protein has received particular attention due to its involvement in the PSII assembly and repair cycle,[4,5] and capability to bind either plastoquinones (PQs) or xenobiotics.[6] The D1 primary structure is highly conserved and the protein folds into five transmembrane α-helices (named from A to E), with their N- and C-termini exposed to the stromal and lumenal sides, respectively. Besides, two short helices occur in the stromal loop, one connecting the membrane spanning helices III–IV (named CD helix), and the other in the lumenal loop connecting helices IV–V (named DE helix). The helices IV and V and their connecting loop integrating the small DE helix build up the Q_B binding niche.[7–9] An *in silico* model of the *Chlamydomonas reinhardtii* D1 protein three-dimensional structure identified a sequence of approx. 70 amino acids, ranging from residue 211 to residue 280, involved in the arrangement of the Q_B pocket, and paved the way to the exploration of its physico-chemical properties by novel computational and engineering methodologies.[8,10,11]

In the agro-food field, the discovery of spontaneous D1 mutations in several weed species survived to the extensive use of the PSII herbicide atrazine,[12] laid a foundation for the rationale use of herbicides, and provided insights into the molecular mechanisms underlying the photosynthetic electron transfer.[13,14] Atrazine competitively inhibits Q_B binding to the D1 protein impairing the natural flux of the electrons to the subsequent acceptors, and inducing an accumulation of the reduced form of Q_A. Acting in a similar manner, other poisonous xenobiotics such as triazinic and ureic herbicides affect the photosynthetic electron transfer.[15,16] This amazing feature of PSII to bind different classes of toxic compounds stimulated the design of analytical devices exploiting the photosynthetic activity of whole cells, or their active subcomponents, as bio-recognition elements.[17,18] In this context, although the use of thylakoidal membranes or isolated protein complexes provides high sensitivity, their extraction, purification or *in vitro* reconstitution procedures are often laborious, expensive and in some cases not always reliable. On the other side, whole cell-based biosensors preserve photosystem functionality, but provide a slow response and sometimes low sensitivity.[19]

The improved resolution of PSII atomic structure from thermophilic cyanobacteria revealed molecular insights into the PSII reaction centre empowering the exploitation of protein engineering tools to fine tune its structural and functional properties.[20–22]

In the nanotechnology era, numerous research efforts have been focused on the design of novel biomimetic molecules able to simulate biological processes, such as the binding of specific analytes.[23,24] These synthetic compounds include peptides, mini-proteins, imprinting polymers or aptamers, and usually derive from a size-minimization strategy, which also aims to fine tune their sensitivity, selectivity, and robustness properties.[25,26] The novel products can be exploited as simplified models to deepen the knowledge of the natural macromolecular functions and as molecular tools finding applications in the development of analytical devices, such as biosensors and biochips.[27–30]

In this work, the *C. reinhardtii* D1 primary structure was used as a template to design new peptides enabling atrazine binding. By computational modeling and automated protein synthesis, the D1 plastoquinone–atrazine binding niche in native and mutated forms was reconstituted and the structural and functional features were analyzed in detail by circular dichroism, fluorescence spectroscopy and microcalorimetry. In particular, the interaction dynamics and the structural stability of the peptides in response to the ligand were considered being mandatory parameters in biosensors/biochips development.

Experimental

Analysis of D1 protein three-dimensional structure and design of the biomimetic peptides

Analysis of the *C. reinhardtii* D1 protein three-dimensional structure was carried out on a previously published molecular model of the *C. reinhardtii* reaction center[6] built using the crystal structure of the *Thermosynechococcus elongatus* reaction center as a template[15] (PDB code 2AXT). Analysis of the model evidenced that the Q_B binding niche is held in place by the interaction between hydrophobic residues located on the two adjacent D and E helices. In particular, a hydrophobic cluster, formed by residue Phe211 on helix D, and residues Phe274, Leu275, Trp278 and Pro279 on helix E, is located just beneath the Q_B binding pocket. Thus, with the aim of preserving these interactions, a first protein minimization was carried out by designing a peptide encompassing the 211–280 region of the D1 protein (named D1pep70). Characterization of the corresponding synthetic peptide revealed its poor solubility (see the Results and discussion section) prompting the addition of two Lys residues at the N-terminus and at the C-terminus of the peptide to increase its solubility. However, notwithstanding the higher water solubility of this second peptide variant, named D1pepLys, CD spectroscopy analysis indicated a low ordered structure content. A third peptide variant was then designed by substituting six Phe residues with Tyr, four Ala residues with Ser (213, 233, 250, and 263), eliminating residues 276 to 280 and adding three Lys residues at both the N- and C-terminal ends of the peptide. This latter peptide variant was named D1pepMut.

Biomimetic peptide synthesis

The peptides were produced by automated synthesis by GenScript Corporation (120 Centennial Ave., Suite 105, Piscataway, NJ 08854, USA). The peptides were synthesized by liquid phase peptide synthesis (LPPS) and solid phase peptide synthesis (SPPS) platforms (FlexPeptideTM), and purified to obtain samples with >90% of purity. The synthetic molecules were analyzed by MS/HPLC and sequence confirmation was performed.

Circular dichroism

Circular dichroism spectra were performed under a nitrogen flow on a J-600 Spectropolarimeter (Jasco, Tokyo, Japan) equipped with the Neslab RTE-110 temperature controlled liquid system

(Neslab Instruments, Portsmouth, NH). Peptide solutions of about 0.2 mg ml^{-1} in 1 mM NaPi buffer pH 7.0 were placed in sealed cuvettes with a 0.05 cm path length (Hellma, Mülheim, Germany), and spectra were measured between 250 and 190 nm with the following setup: bandwidth 1 nm, response 0.25 s, speed 50 nm min^{-1}, sensitivity 20 mdeg, and step resolution 1 nm. All spectra were averaged 16 times and smoothed using the Spectropolarimeter System Software, Version 1.00 (Jasco). Before measurements, all samples were temperature equilibrated for 5 min. During the measurement the photomultiplier voltage never exceeded 600 V. The results were expressed in terms of the molar ellipticity, as previously reported.[31]

Fluorescence spectroscopy

Fluorescence spectra were recorded in 1 mM NaPi buffer, pH 7.0 peptide solutions. Steady-state fluorescence measurements were performed on a F-8200 Spectrofluorometer (Jasco, Tokyo, Japan) with a cell temperature controlled sample holder, equipped with the Neslab RTE-110 temperature controlled liquid system (Neslab Instruments, Portsmouth, NH). Peptide fluorescence was excited at 280 nm, with an emission and excitation slit width of 5 nm. Before measurements, all samples were temperature equilibrated for 5 min.

Quenching

Peptide fluorescence was quenched by acrylamide or sodium iodide and observed at the fluorescence maximum. Steady state quenching was analyzed by the Stern–Volmer equation:

$$\frac{F_0}{F} - 1 = K_{SV}[Q]$$

where F_0 and F are the fluorescence intensities in the absence and in the presence of the quencher, respectively, [Q] is the concentration of the quencher, and K_{SV} the apparent Stern–Volmer constant.[32]

Isothermal titration calorimetry

ITC experiments were performed at 25 °C using a MicroCal ITC200 microcalorimeter (MicroCal Inc., Northampton, MA, USA). The peptide solution (20 μM, in buffer 1 mM PBS pH 7.0, 1% MeOH, 0.1% SDS) was placed in the sample cell, and the ligand solution (200 μM, in the peptide buffer) was loaded into the syringe injector. The titration involved 19 injections of 2 μL at 180 s intervals. The syringe stirring speed was set to 1000 rpm. Reference titration of the ligand into buffer was used to correct for heat of dilution. The thermodynamic data were processed using the Origin 7.0 software provided by MicroCal. Fitting the binding isotherm with the one-site binding model yielded the values of ΔH and of the association constant (K_a). The system also gave information of the change in entropy (ΔS). The inflection point in the isotherm gives the stoichiometry value n, indicating the ligand/peptide ratio of the binding. To correct for any discrepancy in the baseline outlined by the software, a manual adjustment was performed.

Results and discussion

A computational strategy has been adopted for designing and minimizing the Q_B binding domain of *C. reinhardtii* as a receptor for atrazine binding. In particular, we explored by *in silico*/*in vitro* studies, the structure and binding ability of synthetic peptides that could mimic the Q_B–herbicide binding niche of the PSII reaction center D1 protein. The primary sequences of the biomimetic peptides are reported in Table 1.

The *in silico* model of the whole D1 protein from *C. reinhardtii* was preliminary to the actual studies[8] (Fig. 1A). Starting from this point, we have identified a protein sequence, possibly having the proper physico-chemical features to adopt a stable fold, and therefore reproduce the Q_B–herbicide binding niche (highlighted in Fig. 1A). The protein domains were designed to consist of three alpha helices connected by a hydrophilic loop. Hence, we approached the goal of producing synthetic biomimetic peptides by a stepwise optimization of the peptide sequence following experimental analyses of the different peptide variants.

The first peptide, called D1pep70, is a 70 amino acids long peptide corresponding to the native D1 sequence from residue 211 to 280. The *in silico* model of D1pep70 consists of two α-helices at the N-terminal and the C-terminal and a loop of 50 amino acids, which corresponds to the Q_B binding site. The chemically synthesized D1pep70 appeared as a highly hydrophobic molecule soluble only in buffers containing DMSO (20% v/v) and 0.1% (w/v) octyl-glucoside. Due to the presence of such a high concentration of DMSO, any structural analysis of the molecule resulted to be difficult and prone to artifacts (data not shown).

For this reason, a second peptide called D1pepLys was designed by adding two Lys residues at the N- and C-terminal ends of the D1pep70 peptide, in order to increase its solubility in water. The addition of two terminal Lys residues had the additional advantage of facilitating the immobilization of the macromolecule on different organic/inorganic supports by means of covalent attachment.[33] D1pepLys peptide showed a higher solubility in aqueous solvents when compared to D1pep70. This allowed a series of circular dichroism (CD) and fluorescence spectroscopy studies aimed at determining its structural stability and binding capability. However, CD measurements also revealed in this case a poorly structured fold, so we moved one step further and introduced additional changes in the peptide sequence.

The third peptide, called D1pepMut, was obtained by redefining the sequence in order to obtain a new molecule which could be more hydrophilic although maintaining its

Table 1 D1pep70, D1pepLys and D1pepMut sequences. The aminoacidic substitutions are highlighted in yellow

D1pep70	211	FSAMHGSLVT SSLIRETTEN ESANEGYRFG QEEETYNIVA AHGYFGRLIF QYASFNNSRS LHFFLAAWPV	280
D1pepLys	211	KSAMHGSLVT SSLIRETTEN ESANEGYRFG QEEETYNIVA AHGYFGRLIF QYASFNNSRS LHFFLAAWPK	280
D1pepMut	208	KKK YSSMHGSLVT SSLIRETTEN ESSNEGYRYG QEEETYNIVS AHGYFGRLIY QYSSYNNSRS LHYYLAKKK	277

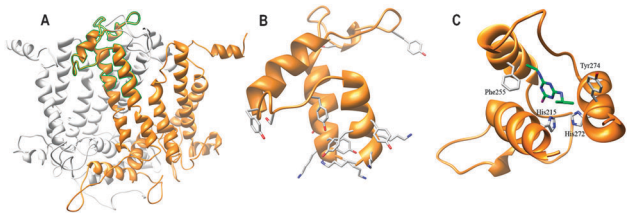

Fig. 1 (A) Schematic representation of the three dimensional structure of the *C. reinhardtii* reaction center (D1–D2 heterodimer). The region corresponding to the peptide is highlighted in green. (B) Structural model of D1pepMut showing the positions mutated with respect to the wild type amino acid sequence. (C) Putative D1pepMut–atrazine complex obtained by docking simulations.

global fold. To this aim, six Phe residues (211, 239, 260, 265, 273, and 274) were substituted with isosteric Tyr residues, four Ala residues (213, 233, 250, and 263) were substituted with more polar Ser residues, and the residues 276–280 (Ala276-Ala277-Trp278-Pro279-Val280) were eliminated; in addition, three Lys residues were added to both the N- and C-terminal end of the peptide. D1pepMut is a 8.4 kDa molecule containing 10 tyrosine residues at positions 211, 237, 239, 246, 254, 259, 262, 265, 273, 274, and a phenylalanine residue at position 255. The predicted three-dimensional structure of the D1pepMut is depicted in Fig. 1B. The structure of the putative complex between D1pepMut and atrazine was modeled through docking simulations using AutoDock Vina program.[34] Fig. 1C shows the lowest energy pose obtained by docking simulations. Indeed in this model atrazine is bound in the Q_B binding pocket even though the search space of the docking simulations encompassed the whole peptide model structure. Atrazine binding is stabilized by hydrophobic interactions with Phe255 and Tyr274, and electrostatic interactions with His215. These computational results were further confirmed by experimental data indicating that D1pepMut adopts a more stable fold in response to atrazine binding as reported below.

Structural investigation of the synthetic peptides

The structure and binding capability of the synthetic peptides D1pepLys and D1pepMut were probed by fluorescence spectroscopy, circular dichroism (CD) and microcalorimetry. The far-UV CD spectra of D1pepLys and D1pepMut at 25 °C are reported in Fig. 2A, whereas Fig. 2B shows the corresponding fluorescence emission spectra. CD spectra indicated that D1pepLys has a higher amount of disordered regions compared to D1pepMut. In particular, the latter has two markedly pronounced negative CD bands between 200 and 220 nm, typical of properly-folded α-helical proteins.[35] Fluorescence emission spectra are in agreement with CD data. D1pepLys contains four Tyr residues at positions 237, 246, 254, 262 located in the Q_B binding niche, giving a shoulder peak at around 310 nm, and one Trp residue at position 278 located in the C-terminal portion of the peptide. The intrinsic emission band of Trp278 is centered at 340 nm, which indicates an indole ring quite exposed to the aqueous medium. Otherwise, the intrinsic emission profile of D1pepMut is characteristic of a peptide lacking Trp residues. The ten Tyr residues produce an emission peak centered at 308 nm, revealing the heterogeneity of the microenvironments of the different Tyr residues which are spread in the whole peptide structure. Either circular dichroism or fluorescence spectroscopy suggests that D1pepMut displays a three-dimensional structure similar to that of the D1 protein region we synthetically reconstructed. For these reasons, the D1pepMut peptide was chosen as a good candidate towards the development of a sensing system for atrazine detection. In the framework of biosensor development for the detection of herbicides exploiting new synthetic molecules, further characterization by fluorescence spectroscopy and microcalorimetry of D1pepMut was carried out to probe its binding ability for atrazine and, in particular, the effect of atrazine binding on peptide conformational properties.

Evidence of Q_B–atrazine binding

The binding ability of D1pepMut towards its natural target analyte was followed by fluorescence spectroscopy. Serial additions of Q_B (0–12 μM concentration range) were supplied to D1pepMut (4 μM), and the peptide intrinsic fluorescence emission intensity due to the Tyr residues was recorded. The samples were excited at 280 nm and the emission was monitored in the

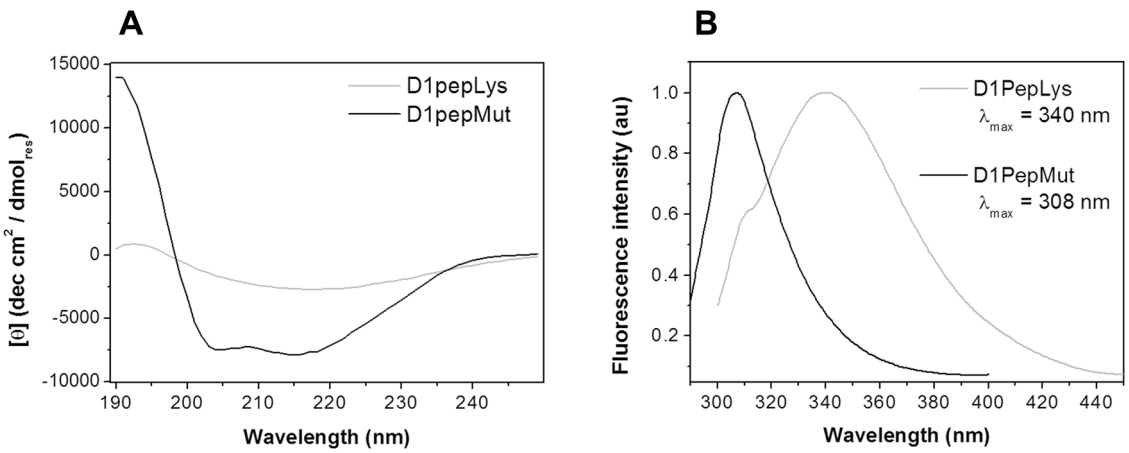

Fig. 2 (A) Far-UV CD spectra of D1pepLys and D1pepMut peptide at 25 °C, in 1 mM PBS pH 7.0, with a peptide concentration of 0.02 mg ml^{-1} and an optical path of 0.5 cm. (B) Normalised steady-state fluorescence emission spectra of D1pepLys and D1pepMut peptide in 1 mM NaPi pH 7.0 (excitation wavelength 280 nm).

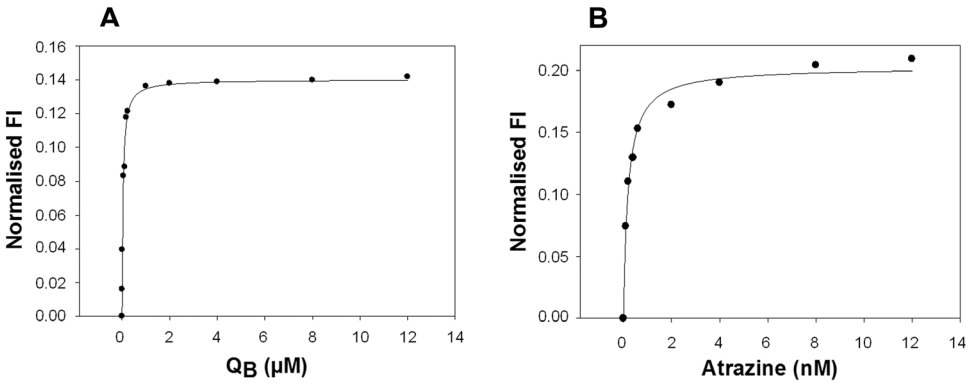

Fig. 3 Fluorescence binding assay of the D1pepMut to (A) the natural ligand Q_B, and (B) the herbicide atrazine.

300 to 450 nm region. The tyrosine emission band decreases as the quinone concentration increases. Corrections were made for dilution of the sample and for a background signal from buffer. The peptide showed high affinity towards Q_B as indicated by the fluorescence binding curve of D1pepMut in the presence of increasing amounts of Q_B in Fig. 3A. To measure ligand binding affinity towards herbicides, serial additions of atrazine (0–12 μM concentration range) were supplied to D1pepMut (4 μM), with the same procedure described above. Fig. 3B shows the fluorescence binding curve of D1pepMut in the presence of increasing amounts of atrazine.

Fluorescence characterization

In depth-fluorescence analyses were performed to shed light on the effect of herbicide binding on the structural stability of the peptide. Variations of the D1pepMut intrinsic fluorescence induced by physico-chemical denaturant agents, such as temperature and guanidinium chloride (GdnHCl), were determined in the absence and in the presence of atrazine (Fig. 4). As shown in Fig. 4A, the fluorescence melting curve of D1pepMut decreases almost linearly in the range 20–95 °C. This transition exhibited very low cooperativity, suggesting that no major structural change takes place in this temperature range. Interestingly, in the presence of atrazine the thermal denaturation appears to be cooperative, giving a sigmoidal profile that fits with a two-state unfolding model. In particular, in the presence of 100 μM atrazine, D1pepMut emission intensity exhibits a modest change up to about 50 °C followed by a steep decrease between 50 and 70 °C, and again a lower slope at higher temperatures. By fitting this curve, a melting temperature (T_M) of 63.8 °C was obtained. This pattern indicates that atrazine induces a conformational change in the D1pepMut structure stabilizing it, so that the tyrosine residues that are directly (or indirectly) affected by its presence display a cooperative transition, as expected by a niche/site of a folded peptide. The chemical denaturation profiles displayed a similar pattern, as shown in Fig. 4B. The intrinsic D1pepMut fluorescence increases as the GdnHCl concentration is raised from 0 to 8 M. The stabilization-by-substrate hypothesis, suggested by the thermal denaturation experiments, is in agreement with the chemical denaturation data presented in Fig. 5B, where the peptide–atrazine complex appears to unfold at substantially higher GdnHCl concentrations than the free peptide.

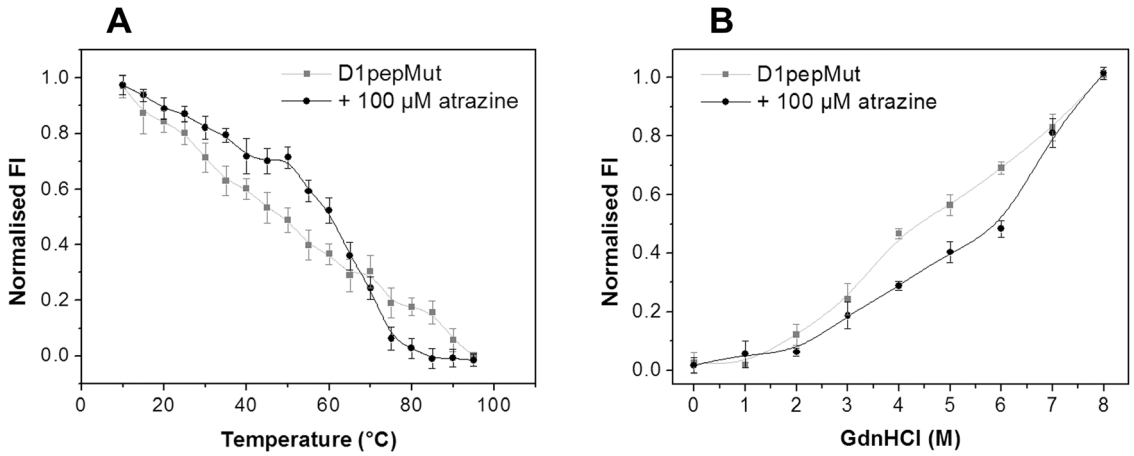

Fig. 4 Thermal and chemical stability of D1pepMut in the absence and in the presence of 100 μM atrazine. (A) Temperature dependence of the emission spectra obtained between 15 and 95 °C at 5 °C increments. (B) GdnHCl concentration dependence of the emission spectra in the range of GdnHCl concentration 0.0–8.0 M. The fluorescence intensities were measured at the emission maximum.

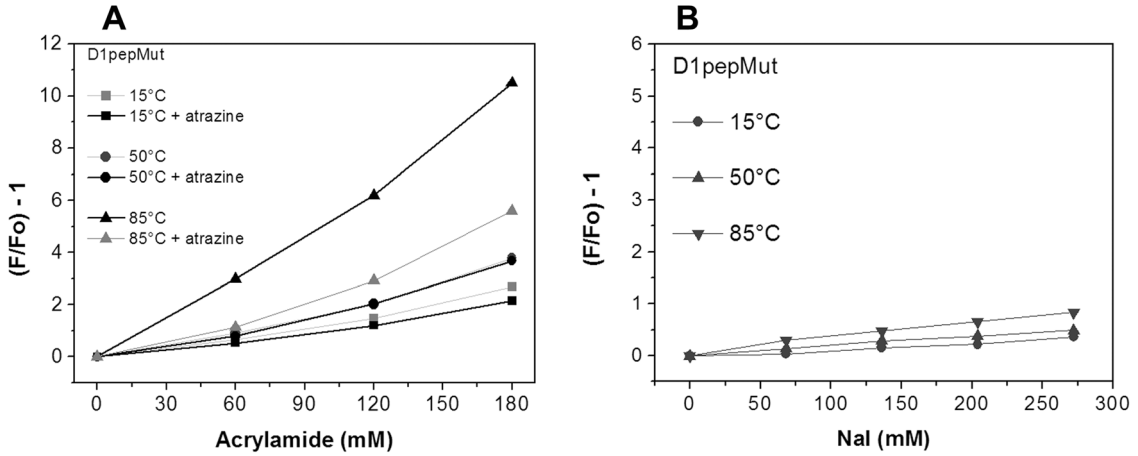

Fig. 5 (A) Effect of acrylamide and (B) NaI on the fluorescence emission of the D1pepMut peptide in the absence and in the presence of atrazine at 15, 50, 85 °C.

Fluorescence quenching

Next, we reasoned that collisional quenching experiments might shed light on the fold and binding ability of D1pepMut, due to selective interactions of the quenchers with exposed Tyr residues. To this purpose, we used acrylamide and NaI at different temperatures (15, 50, 85 °C), in the absence and in the presence of atrazine. The Stern–Volmer plot[32] for acrylamide quenching is given in Fig. 5A. The slope of the curves, and the Stern–Volmer constant K_{SV}, indicates the effectiveness of the quencher to reduce the protein fluorescence. The increase of the Stern–Volmer slope with the temperature (Table 2) indicates that the acrylamide accessibility to Tyr residues, as expected, increases with temperature. A steep increase is observed at 85 °C, indicating a dramatic structural rearrangement of D1petMut at this temperature. Interestingly, in the presence of atrazine, we registered only small variations at 15 and 50 °C, while a markedly reduced quenching is observed at 85 °C. In particular, at this temperature, acrylamide quenching ability is reduced by 50% when compared to the experiment in the absence of atrazine. This result indicates that atrazine interacts with the D1pepMut so that about 50% of the acrylamide-sensitive tyrosines were effectively shielded. This reduced efficiency in penetrating the protein matrix and quenching the aromatic residues highlights large structural effects due to the presence of the ligand atrazine.

In the presence of NaI, which is a quencher not capable of entering deeply in the protein structure,[36] Stern–Volmer slopes are lower than the corresponding values recorded for acrylamide quenching (Fig. 5B). Their numerical values, also shown in Table 2, suggest that a fraction of the ten tyrosine residues present in the molecule are exposed to the solvent. These residues are probably not involved in atrazine binding, because the effectiveness of their quenching smoothly increases with temperature and do not show the abrupt change (as in the case of acrylamide/high temperature quenching).

Table 2 Stern–Volmer quenching constants (K_{SV}) of the D1pepMut peptide in the absence and in the presence of atrazine at 15, 50, 85 °C

		K_{SV} (M^{-1})		
		15 °C	50 °C	85 °C
Acrylamide	−Atrazine	12.0 ± 0.3	16.4 ± 0.4	51.2 ± 0.4
	+Atrazine	9.9 ± 0.3	16.3 ± 1.1	23.4 ± 1.5
NaI	−Atrazine	1.2 ± 0.1	1.9 ± 0.1	3.2 ± 0.1
	+Atrazine	1.3 ± 0.1	1.8 ± 0.1	3.4 ± 0.1

Microcalorimetry

With the aim to confirm and characterize the peptide–ligand binding we decided to perform isothermal titration calorimetry[37] (ITC) experiments. This technique allows us to measure the thermodynamic parameters associated with the formation of the complex peptide–atrazine. Particularly, by measuring the heat absorbed or released by titrating the peptide with a ligand

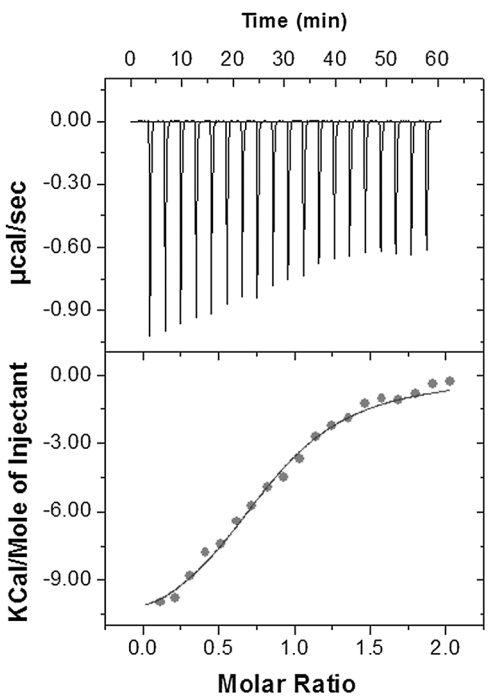

Fig. 6 Isothermal titration calorimetry experiments of D1pepMut interacting with atrazine. Raw data (upper panel) and integration data (lower panel).

at constant temperature it is possible to obtain the stoichiometry of the reaction, the binding enthalpy and the affinity constant. Fig. 6 shows the calorimetric data (raw and integration data) obtained in the titration of D1pepMut with atrazine. After subtraction of the heat of dilution from the raw data and linear curve fitting under the ''one binding site'' model the thermodynamic parameters shown in the lower panel of Fig. 6 were obtained. Atrazine binds to the peptide with an affinity constant of 3.52×10^5 M^{-1} (K_d = 2.84 μM). The stoichiometric n value (n = 0.86) corresponds to a 1 : 1 binding mode. Despite a very unfavorable entropic term ($-T\Delta S$ = 4.3 kcal mol^{-1}), the favorable enthalpic contribution ($\Delta H = -11.9$ kcal mol^{-1}) leads to a net negative free energy value of −7.6 kcal mol^{-1}, suggesting an enthalpy driven reaction with productive interactions between peptide and atrazine. The loss of entropy could be ascribed to a more ordered and stable structure of the peptide upon ligand binding.

Conclusions

The increasing knowledge of biological natural molecules continuously challenges and stimulates the design of novel and artificial materials with similar biomimetic properties. The recent progress in molecular engineering and nanotechnology witnesses the great interest to create novel molecular structures *de novo* or by rational design. In particular, the development of biomimetic peptides and small proteins is an expanding area in this research field, which will pave the way to a vast area of future applications.[38]

In this paper we described the first attempt to create novel D1-inspired biomimetic molecules with high potential applications in the realization of nanosensor arrays for the detection of herbicides. The synthesized biomimetic molecules were deeply characterized and their structural and functional features studied in response to atrazine binding. In this context, we reported that atrazine binding induces extensive changes in the peptide molecules, resulting in a more stable structure as indicated by fluorescence measurements. We have also documented that D1pepMut shows a high affinity towards atrazine, detecting the herbicide in the micromolar range. Taken together, these results showed that peptides could represent an important alternative as recognition molecules, exhibiting high sensitivity towards target analytes, without the stability and reliability weaknesses often associated with entire native proteins. Future efforts will be dedicated to further improve the peptide binding affinity towards atrazine, as well as to deliver a library of peptide variants with increased selectivity and sensitivity headed for a wide range of herbicides. This achievement will pilot the design of a nanosensor array of biomimetic molecules with different specificities for different chemical species, making these molecules a useful tool as probes in the development of last generation of biosensing systems.[39]

Acknowledgements

This work was supported by the FP7-SME-2008-1 SENSBIOSYN project (ID: 232082, http://www.sensbiosyn.com), the Filas MICROBIOSIS project, and the COST Action TD1102 PHOTOTECH (http://www.phototech.eu).

Notes and references

1 J. Barber, *Biochem. Soc. Trans.*, 2006, **34**, 619.
2 T. Wydrzynski and K. Satoh, in *Advances in Photosynthesis and Respiration*, ed. Govindjee, Springer, 2005, p. 11.
3 G. Renger and T. Renger, *Photosynth. Res.*, 2008, **98**, 53.
4 J. Komenda, R. Sobotka and P. J. Nixon, *Curr. Opin. Plant Biol.*, 2012, **15**, 245.
5 P. J. Nixon, F. Michoux, J. Yu, M. Boehm and J. Komenda, *Ann. Bot.*, 2010, **106**, 1.
6 M. D. Lambreva, M. T. Giardi, I. Rambaldi, A. Antonacci, S. Pastorelli, I. Bertalan, U. Johanningmeier and G. Rea, *PLoS One*, 2013, **8**, e61851.
7 J. Xiong, S. Subramaniam and Govindjee, *Protein Sci.*, 1996, **5**, 2054.
8 G. Rea, F. Polticelli, A. Antonacci, V. Scognamiglio, P. Katiyar, S. A. Kulkarni, U. Johanningmeier and M. T. Giardi, *Protein Sci.*, 2009, **18**, 2139.
9 Y. Umena, K. Kawakami, J.-R. Shen and N. Kamiya, *Nature*, 2011, **473**, 55.
10 G. Rea, F. Polticelli, A. Antonacci, M. Lambreva, S. Pastorelli, V. Scognamiglio, V. Zobnina and M. T. Giardi, in *Herbicides, Theory and Applications*, ed. S. Soloneski and M. L. Larramendy, 2011, p. 5.
11 Z. Perrine and R. Sayre, *Biochemistry*, 2011, **50**, 1454.
12 J. Hirschberg, A. B. Yehuda, I. Pecker and N. Ohad, in *Plant Molecular Biology*, ed. D. von Wettstein and N.-H Chua, Plenum Press, New York, 1987, p. 357.
13 A. Trebst, *Z. Naturforsch.*, 1987, **42**, 742.
14 C. Sundby, W. S. Chow and J. M. Anderson, *Plant Physiol.*, 1993, **103**, 105.
15 S. B. Powles and Q. Yu, *Annu. Rev. Plant Biol.*, 2010, **61**, 317.
16 R. Takahashi, K. Hasegawa, A. Takano and T. Noguchi, *Biochemistry*, 2010, **49**, 5445.
17 M. Kato, T. Cardona, A. W. Rutherford and E. Reisner, *J. Am. Chem. Soc.*, 2012, **134**, 8332.
18 F. Milano, R. R. Tangorra, O. H. Omar, R. Ragni, A. Operamolla, A. Agostiano, G. M. Farinola and M. Trotta, *Angew. Chem., Int. Ed.*, 2012, **51**, 11019.
19 V. Scognamiglio, G. Pezzotti, I. Pezzotti, J. Cano, K. Buonasera, D. Giannini and M. T. Giardi, *Microchim. Acta*, 2010, **170**, 215.
20 B. Loll, J. Kern, W. Saenger, A. Zouni and J. Biesiadka, *Nature*, 2005, **438**, 1040.
21 F. Müh, W. Saenger and A. Zouni, *ChemPhysChem*, 2010, **11**, 1160.
22 A. Guskov, J. Kern, A. Gabdulkhakov, M. Broser, A. Zouni and W. Saenger, *Nat. Struct. Mol. Biol.*, 2009, **16**, 334.
23 K. H. Smith, E. Tejeda-Montes, M. Poch and A. Mata, *Chem. Soc. Rev.*, 2011, **40**, 4563.
24 C. Tamerler and M. Sarikaya, *Acta Biomater.*, 2007, **3**, 289.
25 S. Lagziel-Simis, N. Cohen-Hadar, H. Moscovich-Dagan, Y. Wine and A. Freeman, *Curr. Opin. Biotechnol.*, 2006, **17**, 569.

26 M. Sarikaya, C. Tamerler, A. K. Jen, K. Schulten and F. Baneyx, *Nat. Mater.*, 2003, **2**, 577.
27 S. Li, Y. Ge, S. A. Piletsky and A. P. F. Turner, *Adv. Funct. Mater.*, 2011, **21**, 3344.
28 Y. Bar-Cohen, *Int. J. Aeronaut. Space Sci.*, 2012, **13**, 1.
29 R. K. Mishra, R. B. Dominguez, S. Bhand, R. Munoz and J.-L. Marty, *Biosens. Bioelectron.*, 2012, **32**, 56.
30 M. T. Giardi, V. Scognamiglio, G. Rea, G. Rodio, A. Antonacci, M. Lambreva, G. Pezzotti and U. Johanningmeier, *Biosens. Bioelectron.*, 2009, **25**, 294.
31 P. Herman, J. Vecer, V. Scognamiglio, M. Staiano, M. Rossi and S. D'Auria, *Biotechnol. Prog.*, 2004, **20**, 1847.
32 S. D'Auria, M. Rossi, G. Barone, F. Catanzano, P. Del Vecchio, G. Graziano and R. Nucci, *J. Biochem.*, 1996, **120**, 292.
33 A. Kumar and S. Garg, in *Biotechnology Applications*, ed. C. S. K. Mishra, IK International, New Delhi publisher, 2009, p. 39.
34 A. Trott and J. Olson, *J. Comput. Chem.*, 2010, **31**, 455.
35 R. W. Woody, A. K. Bunker and G. D. Fasman, in *Circular Dichroism and the Conformational Analysis of Biomolecules*, ed. G. D. Fasman, Plenum, New York, 1996, vol. 85, p. 391.
36 J. R. Lakowicz and G. Weber, *Biochemistry*, 1973, **12**, 4171.
37 S. Leavitt and E. Freire, *Curr. Opin. Struct. Biol.*, 2001, **11**, 560.
38 A. Tiwari, A. K. Mishra, H. Kobayashi and A. P. Turner, *Intelligent nanomaterials*, Wiley-Scrivener, 2012.
39 Y. Cui, S. N. Kim, R. R. Naik and M. C. McAlpine, *Acc. Chem. Res.*, 2012, **45**, 696.